Effects of nonlinear elaborations on the performance of a Reichardt correlator

Sreeja Rajesh a,b,c , David O'Carroll a,b,c and Derek Abbott a,c

^aSchool of Electrical & Electronic Engineering, The University of Adelaide, SA 5005, Australia.

^bSchool of Molecular and Biomedical Science, The University of Adelaide, SA 5005, Australia.

^cCentre for Biomedical Engineering, The University of Adelaide, SA 5005, Australia.

ABSTRACT

Flying insects are capable of performing complex and extremely difficult navigational tasks at high speeds with amazing ability. The neural computations underlying these complicated maneuvers and the motor activity of the insects have been extensively investigated in the last few decades.^{1–5} One the most important discovery was that the motion detectors involved in the control of the optomotor responses are of the correlation type.⁶ In order to improve the velocity estimation by the Reichardt correlators, many scientists have come up with different kinds of elaborations to the basic Reichardt correlator model.

In this paper, we have expanded the Dror's elaborated Reichardt model⁷ and we have included feedback adaptation and saturation in our model and we have conducted a comparative study on the effects of the addition of each elaboration on the performance of the model. The relative error in each case is also studied.

1. INTRODUCTION

The ability of insects to perform complex navigational tasks is due in part to its highly efficient and simple visual system. The study of the insect visual system has offered solutions to problems of computational bottleneck and other problems faced by the conventional machine vision algorithms and has led to many elegant strategies that can be profitably applied to motion detection, velocity estimation and has even be used in the design of collision avoidance sensors and autonomous robots.⁴ Research over several decades has revealed that the visual system of insects is exquisitely sensitive to both whole field optic flow and small target motion, inspiring many models of motion detection.^{3,8-11}

One of the earliest and the most prominent models of motion detection is the Reichardt correlator model.⁶ The Reichardt correlation motion detector possess a highly parallel architecture. Each elementary motion detector (EMD) detects motion in a preferred direction by comparing a signal from one receptor with a delayed signal from an adjacent receptor. The comparison is performed using a nonlinear, multiplicative interaction between the two channels. Two EMDs tuned to opposite directions are subtracted to form a bidirectional motion detector.

Several authors have proposed elaborations of the 'basic' Reichardt detector by either adding temporal, spatial or spatio-temporal filters before applying the input to the EMD cell.^{12,13} In one of the most recent elaborations of this model, Dror,¹⁴ suggests that the inclusion of additional system components to perform pre-filtering, response compression, integration and adaptation to a basic Reichardt correlator can make it less sensitive to contrast and spatial structure, thereby providing a more robust estimate of local image velocity.

Further author information: (Send correspondence to Sreeja Rajesh) Sreeja Rajesh: e-mail: srajesh@eleceng.adelaide.edu.au, Telephone: 8303-6296

David O'Carroll: e-mail: david.ocarroll@adelaide.edu.au Derek Abbott: e-mail: dabbott@eleceng.adelaide.edu.au

BioMEMS and Nanotechnology, edited by Dan V. Nicolau, Uwe R. Muller, John M. Dell, Proceedings of SPIE Vol. 5275 (SPIE, Bellingham, WA, 2004) 0277-786X/04/ $$15 \cdot doi: 10.1117/12.525433$

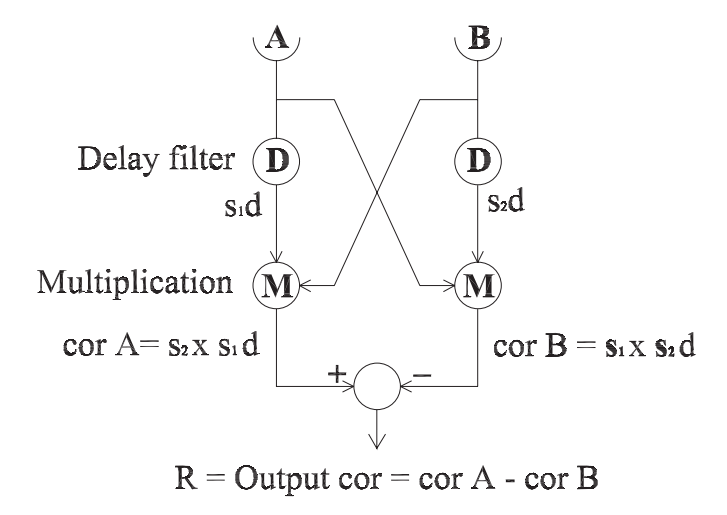


Fig. 1. The Reichardt correlator has two arms A and B. Each of the two time dependent inputs s_1 and s_2 has a fixed angular separation $\Delta \phi$, and pass through a linear delay filter (D) before being multiplied by the other, undelayed signal. The results of the two correlations thus obtained cor A and cor B are subtracted to produce a single output cor. An object moving to the right will produce a positive output; an object moving to the left will produce a negative output.

In this paper, we have extended Dror's model to include two nonlinear elaborations, (i) adaptive feedback and (ii) saturation. We have investigated the effect of each of these elaborations on the performance of our model. It is seen that the addition of these elaborations reduces the dependence of the response on contrast and helps to maintain a good signal to noise ratio.

2. SIMPLE REICHARDT CORRELATOR MODEL

Fig. 1 shows a simplified version of the Hassenstein and Reichardt correlator model. Both behavioural and physiological experiments on the insect visual system indicate that movement detection occurs between neighbouring points of the sampling lattice of the eye. This implies that a motion detector has two input channels and the two channels should possess an asymmetric arrangement. Asymmetry is necessary for the detector to acquire direction selectivity. Furthermore the interaction between two channels must be nonlinear if the detector is to respond selectively to moving gratings. The asymmetrically nonlinear interaction between two input channels will elicit a strong response when a visual stimulus moves in a specified direction (the preferred direction) and weak response when the stimulus moves in the opposite direction.

Elementary motion detector (EMD) is formed by subtracting two such correlators that are tuned to opposite direction, to indicate bidirectional motion. The nonlinear interaction is assumed to be a multiplication, M, which is the simplest possible nonlinear interaction. The asymmetry is implemented by using a delayed unit, D, which is usually a first order low pass filter. This filter acts as a delayed element by introducing phase shift of up to 90°. The input channels are spatially separated by an angular distance, $\Delta \phi$. The delay filter D determines the temporal frequency tuning and therefore the response to different motion velocities at any given spatial frequency. The outputs of the two multiplications are subtracted to give a single time-dependent correlator output.

Though insects and humans appear to be capable of estimating image velocities, ^{15, 16} the basic correlator model does not function as a velocity estimator. It reliably indicates directional motion of sinusoidal gratings, but the response depends on contrast (brightness) and spatial frequency (shape) as well as velocity.⁵ Furthermore, since the EMD is a complex spaiotemporal bandpass filter, any one pattern produces same response at two unique velocities.

Proc. of SPIE Vol. 5275

3. ELABORATED REICHARDT CORRELATOR MODEL

Although the simple correlator model produces more meaningful estimates of velocity for natural images than for arbitrary sinusoids, it suffers from two major shortcomings. First, the standard deviation of the correlator output is huge relative to its mean, typical values values ranging from 3.3 to 76 times the mean. Second, the mean correlator response for most natural images peaks at a velocity of $35-40^{\circ}/\mathrm{s}$ depending on the spatial and temporal filters. Analysis and simulations suggest that the processes commonly found in visual systems, such as pre-filtering, response compression, integration, and adaptation, improve the reliability of velocity estimation and expand the range of velocities coded. Based on these studies we have elaborated the Reichardt correlator model to include various additional components in order to improve its performance as a velocity estimator. The various additions and their functions are described in the forthcoming sections.

4. RELATIVE ERROR

The errors considered here in this paper are due to 'pattern noise', the deviation in correlator output that results from the structure of the visual scene. Physiological motion detectors also suffer from random noise, which is due to the variation in its response on repeated presentation of identical stimulus patterns. The random noise experienced by a biological motion detector falls into two categories, namely photon noise and intrinsic noise. The photon noise results from variations in the number of photons absorbed by a photoreceptor in a given unit of time. In addition, the neurons and synapses that comprise the correlator generate intrinsic noise. Studies done on the LMCs (Lamina Monopolar Cells) by Laughlin¹⁸ indicates that photon noise dominates intrinsic noise up to moderate light intensities and at higher light intensities, photon noise equals intrinsic noise in magnitude.

Dror conducted studies on photon noise using natural images and found that while photon noise leads to a slight increase in relative error, its contribution is small compared to that of pattern noise, suggesting that the performance of a velocity estimation system based on Reichardt correlators is limited primarily by pattern noise. 14

The error measure used here called the relative error defined by Dror as, $E_{rel} = E_{abs}/\overline{R}$, where the absolute error (E_{abs}) is the difference between the actual response and the expected response.¹⁴ The expected response is the mean response value that is given by \overline{R} . For a given set of images, moving at a given velocity, the mean response \overline{R} is calculated by averaging the response of the wide field correlator at all points in the selected sampled space and sampled time. The relative error for the same set of responses is found by dividing their standard deviation by the mean. In this paper, we evaluated the performance of the model based on its effect on pattern noise.

5. STIMULUS TO OUR MODEL

Natural images are not arbitrary. Certain image statistics are highly predictable in the natural world^{7, 23} and the biological visual system is optimized to take advantage of these statistics.¹⁸ The similarities between natural image power spectra lead to predictable peak response velocities and to similarities in the shapes of the velocity response curves for different natural images. The primary difference between the curves, their overall amplitude, results from contrast differences between images. In order to use mean correlator response as a reliable indicator of velocity, the visual system needs to compensate for these contrast variations.¹⁴ In order to decrease the dependance of the response to differences in contrast we have investigated the effect of two nonlinear additions to the model, saturation and contrast adaptation.

In our experiments, natural images photographed from favored hovering positions of the hoverfly are used to obtain panoramic images which are use as stimuli. A panorama is formed by 'warping' 12 image 'tiles' at 30° intervals to remove lens distortion, and then wrapping the ends together using Apple Quicktime VR Authoring Studio. Panoramic images used as stimuli in our experiments are shown in Figure 2.

Image 1



Image 2



Image 3



Image 4



Figure 2. The panoramic natural images given as stimulus to the EMD model. A panorama of the image is formed by 'warping' 12 image tiles at 30° intervals to remove lens distortions and then by wrapping its ends together using Apple Quicktime VR software on a Macintosh computer.

6. ROLE OF ADDITIONAL COMPONENTS ON THE PERFORMANCE OF OUR MODEL

6.1. Spatial prefiltering

Studies on phototransduction in insects reveal that the retinal signal, as sampled by the photoreceptors, is already blurred by diffraction effects of the lens optics as well as the properties of the photoreceptor themselves.²⁴ Hence the response of the photoreceptor to an input image has the characteristics of spatial low pass

Proc. of SPIE Vol. 5275

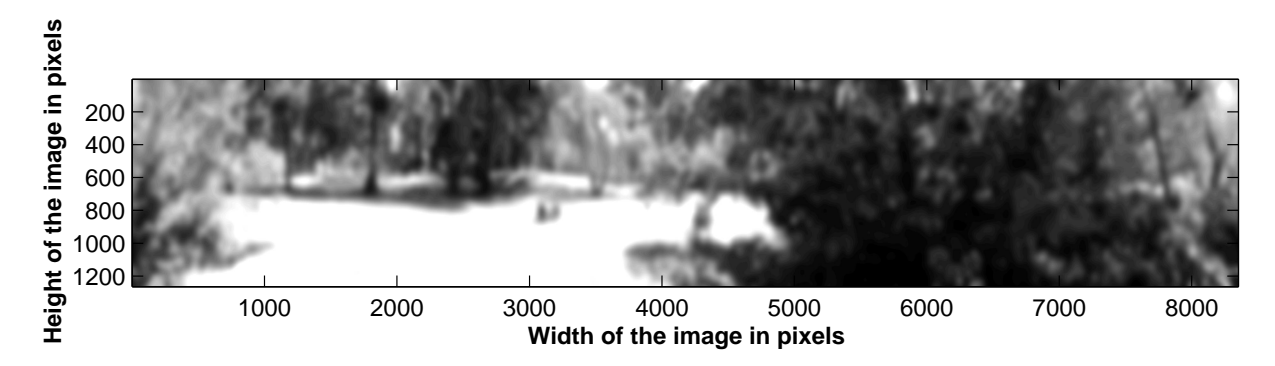


Figure 3. The natural image is pre-filtered using a spatial low pass filter, imitating the characteristics of the photoreceptor. The spatial filter used here is a Gaussian filter of half width 2° . This figure shows the Gaussian filter applied to Image 1.

filter. Studies and analysis by Dror¹⁴ suggests that low pass spatial filtering dramatically decreases the relative error of the correlator particularly at lower velocities. But at higher velocities, the relative error rises even in the presence of spatial filtering because spatial frequencies passed by the pre-filter generate high-frequency inputs to the correlator. The spatial low pass filters are found to raise the peak response velocity. Based on these studies, we have implemented a spatial low pass filter in our model. While some LMCs also appear to perform spatial high-pass filtering of their inputs the phenomenon is weaker and more variable than high pass temporal filtering.^{18, 25}

Spatial pre-filtering in our model is implemented by two-dimensional convolution of the image with a Gaussian kernel of half width of 2°, which approximates the acceptance function of typical fly photoreceptor. Only the luminance (grey scale) information is taken from the image using the green channel, since photoreceptors are green sensitive. The spatially low pass filtered image is illustrated in Figure 3. The distance between two ommatidia in an insect eye is between 1 and 1.5 degrees. Since the insect is looking at an image of 360 degrees, if we consider the inter-ommatidial angle as 1.5 degrees, there will be a total of 240 ommatidia looking at the image. So there will be an array of typically 240 EMDs working together to detect motion.

6.2. Temporal pre-filtering

At very high velocities, the relative error begins to rise even in the presence of spatial pre-filtering, because the spatial frequencies passed by the pre-filter generate high temporal frequency inputs to the correlator while the steady state (DC) response declines due to the low pass nature of the EMD delay filter. Temporal pre-filtering which filters out such frequencies regardless of velocity, serves to reduce the relative error at very high motion velocities. The temporal low pass filtering is found to lower the peak response velocity where as high pass temporal filtering shifts the velocity response to the right, raising the peak velocity.¹⁴

Photoreceptors, which provide the inputs to the correlator, depend on chemical transduction processes that cannot respond instantly to changes in the luminance signal. They therefore filter their inputs with a temporal response found to experimentally to have a log-normal form.²⁷ In addition, there is clear evidence that some kind of temporal highpass filtering takes place in the lamina.^{18, 25} Recordings and modelling by James^{25, 28} from the temporal impulse responses of LMCs (in the hoverfly *Eristalis*), reveals that the LMCs have the characteristic of the difference of two log-normal functions. Addition of this temporal band pass filter is found to increase the peak response velocity and reduce the variance of the correlator output.¹⁴

Hence in our experiments, the image in Figure 3 is temporally filtered with a difference of log-normal filter to copy the response of the lamina monopolar cells. ^{25, 27, 29} The temporally pre-filtered image is converted to a space-time matrix as shown in Figure 4 based on desired velocity, which is then simulated along the height of the image in pixels. The height of the image is also divided into 36 ommatidia by calculating the pixels per

degree and keeping the inter-ommatidial angle as 1.5 degrees. Then this spatio-temporally pre-filtered image is given to the EMD array, which correlates the inputs to give an array of outputs as is postulated to be done in the insect eye. 2,30

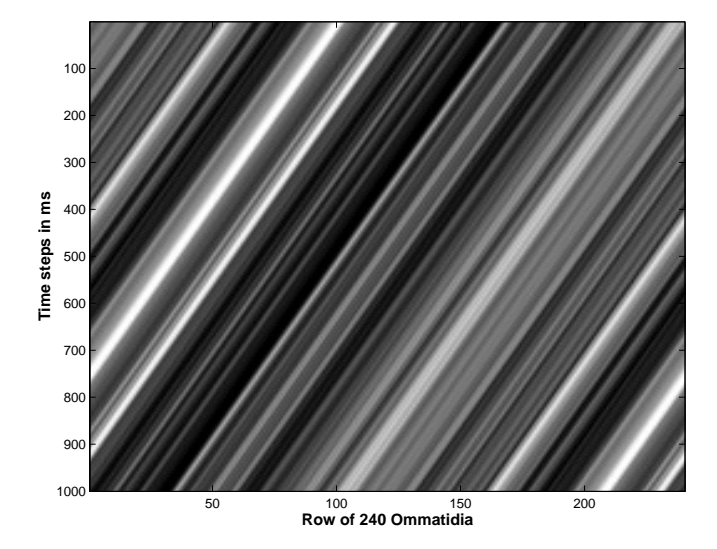


Figure 4. The panoramic image is rotated at a given velocity and is sampled on to an array of 240 EMDs separated by an inter-ommatidial angle of 1.5 degrees. The sample rate used here is 500 samples per second and the duration of the simulation is 2 seconds. The figure shows the image of the space time distribution or the spatio-temporal structure of a simulated single row of the image animated at a given velocity and sampled onto an array of 240 EMDs. Here the image used is image 1 (shown in Figure 9) moving at a constant velocity of 200 degrees per second.

6.3. Output Integration

Integration in space or time has been extensively used to produce reliable motion signals.^{2,31–34} Integration involves a tradeoff between accuracy of velocity estimation and resolution in space and time. In insects, the lobula which contains wide field directionally selective motion detection neurons are responsible for the detection of whole field or whole frame motion. In the lobula, the output of the local retinotopic movement detectors is pooled. This is accomplished in the dendrites of the tangential cells in the lobula plate.² Intracellular recordings from the wide field cells indicate that they sum the outputs of local Reichardt correlators in their receptive fields.⁵ Integration is found to lower the relative error by decreasing the variance of the output signal. It is seen that the decrease is more significant in the presence of saturation.¹⁴

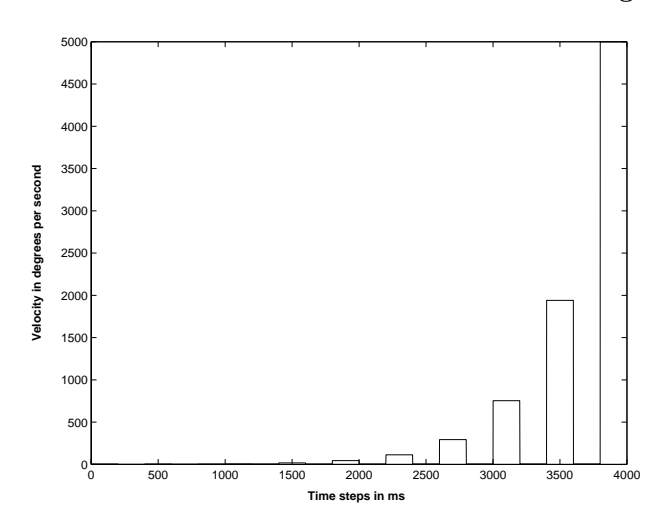
Our EMD array model copies the lobula by averaging the outputs to produce an average EMD response. The simulations are performed by increasing the velocity in steps and the spatial average or the average response of all the EMD rows is shown in Figure 5. Figure 6 shows the mean relative of an elaborated EMD array with spatial and temporal pre-filtering (spatial low pass filter and temporal band pass filter) with the response averaged over 4 images, at 5 different speeds.

6.4. Adaptation

When you observe a fly hovering near a flower, you will be struck by the ability of its visual system to estimate self-motion in order to achieve stabilization during hovering, which shows its sensitivity to low velocities. Similarly when you watch these insects engaging in high speed aerial pursuits while chasing mates, it is clear that their visual system adapts easily to higher velocities as well. These activities of insects demand a visual system with a large dynamic range. Although physiological recordings demonstrate that insect motion detectors have such high sensitivity to contrast that they are able to respond over a huge range of velocities, this inherently high sensitivity to motion makes them prone to saturation^{22,35}

Proc. of SPIE Vol. 5275





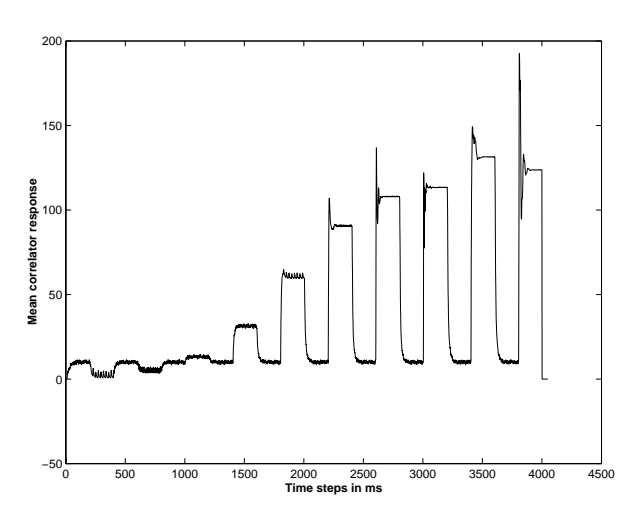


Figure 5(a). To test motion adapted responses, we increased velocity step-wise, with interleaved bursts of adapting motion (constant speed). The adapting speed used here is low (5 degrees per second). The velocity is increased in steps with time.

Figure 5(b). The mean correlator simulated response of the EMD array model to a natural image moving with velocity increasing in steps across the EMD array.

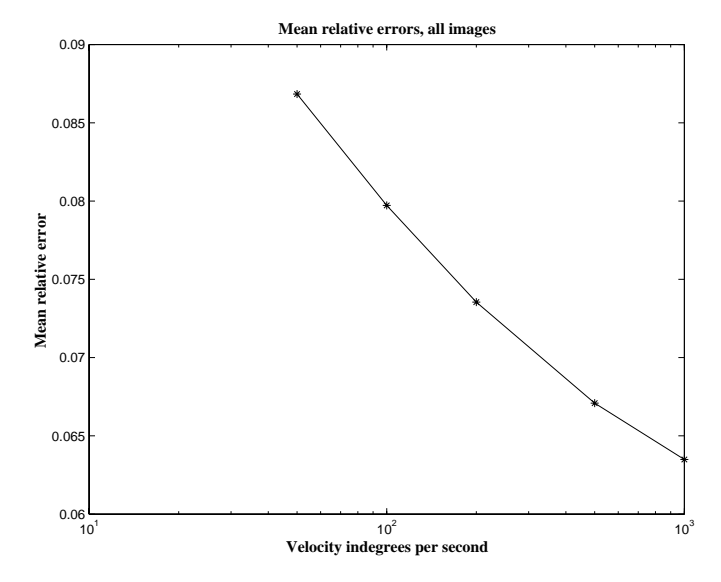


Fig. 6. This figure shows the simulated mean relative error of elaborated EMD array model with spatial and temporal pre-filtering with the response averaged over 4 images, at 5 different speeds. The relative error is found to decrease with increase in velocity.

Recent studies in the fly by Harris $et~al~(1999)^{22}$ show little change in the temporal and spatial tuning properties of fly motion sensitive cells following adaptation, indicating that motion adaptation does not significantly alter the inherent velocity optimum of the EMDs. Instead this work reveals that motion adaptation induces a profound decrease in contrast sensitivity of fly motion sensitive cells via two proposed mechanisms, a

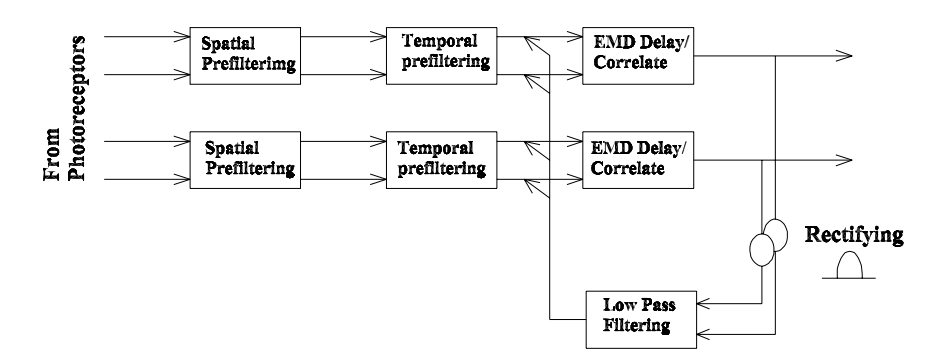


Figure 7. Block diagram of a feedback adaptive EMD model. In this model, the output of the correlator is rectified and low pass filtered and is fed back to control the gain of the EMD inputs.

local direction sensitive after potential and a local direction insensitive contrast control. We propose that this gain reduction may serve to reduce sensitivity to image contrast, as well as reducing tendency of the motion detectors to saturate.

7. ELABORATED EMD MODEL WITH ADAPTATION

In our elaborated Reichardt correlator array model, in order to reduce the dependency of the response to changes in contrast and spatial frequency and to get a more accurate estimate of velocity, contrast gain reduction is implemented as a dynamic non-linearity in which the EMD output is fed back to control the input gain as in Figure 7. The gain of the EMD inputs is reduced by a signal derived from the rectified and low pass filtered outputs of a local EMD pool with different local preferred direction. The model was inspired by recent observation of contrast dependent gain reduction in the responses of HS neurons following motion stimulation.³⁵ The model captures several aspects of the adaptive phenomena observed in the biological system. In particular, the adaptation is strongest when the local motion detector output is the largest, conferring a robustness in adaptation to motion signals as opposed to static flicker or noise applied to the inputs. This matches data obtained from the electrophysiological experiments, which show that motion stimuli are much more effective at recruiting adaptive gain reduction than other stimuli.³⁵ Secondly, the adaptive mechanisms remain independent of the direction of local motion, despite the selectivity for motion as the source of adaptation.

In order to test the performance of this adaptive EMD array regarding contrast, we have compared the responses of the non-adapted elaborated EMD array with the adaptive elaborated EMD array at three different contrasts. From the graphs (Figure 8 and Fig 9) it is very clear that the adaptive feedback mechanism has resulted in decreasing the contrast sensitivity of the model, compared with an otherwise similar model that lacks adaptive feedback. It is also found that the adaptation is stronger at higher velocities and at higher contrasts.

The simulated relative error of this adaptive EMD array model is then compared to that of the non adaptive-elaborated EMD array model as shown in Figure 10. The relative error of one row of the EMD array of the elaborated EMD model with adaptation is compared to that of the elaborated EMD model without

294 Proc. of SPIE Vol. 5275

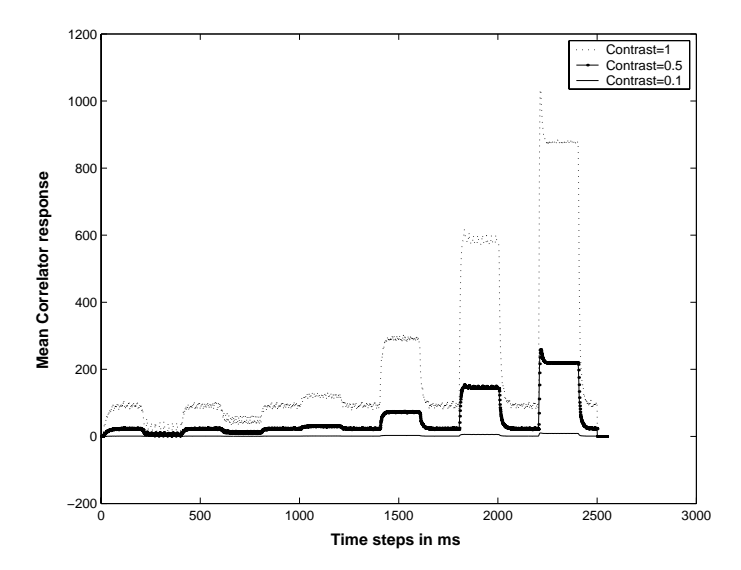


Fig. 8. The simulated mean correlator response of one row of an non-adapting EMD array at three different contrasts. The response of the elaborated EMD array without including the adaptive feedback loop is noted at three different contrast (1, 0.5 and 0.1). It is clearly seen from the graph that there is huge variation of the response with contrast.

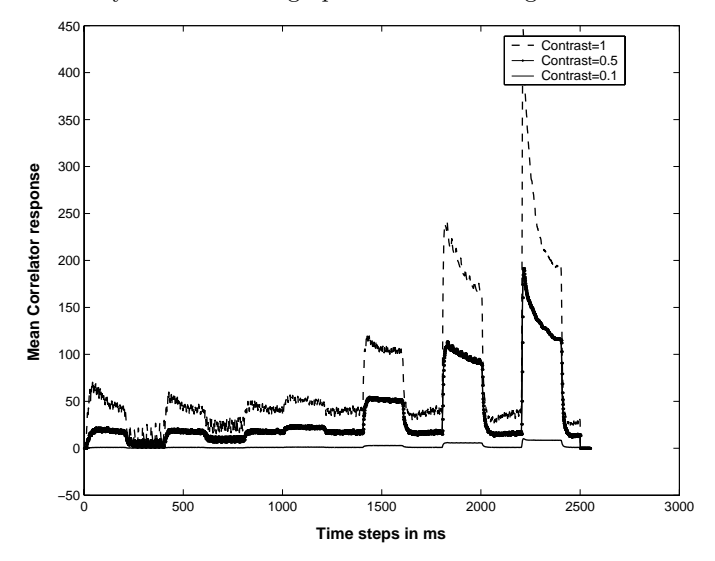


Fig. 9. The simulated mean correlator response of one row of an adaptive EMD array at three different contrasts. The response of the elaborated EMD array including the adaptive feedback loop is noted at three different contrast (1, 0.5 and 0.1). The adaptive feedback mechanism helps in decreasing the dependence of the response to contrast.

adaptation. It is seen that even though adaptation reduces the dependence of the response to contrast, it increases the relative error and the relative error increases with increase in the velocity because adaptation introduces more variation in the correlator response and hence more errors at higher velocities. Figure 11 shows the simulated mean relative error of total elaborated EMD array with adaptation with the response averaged over 4 images, at 5 different speeds. It is also seen from both the figures that output integration or averaging of all the rows of EMDs reduces the relative error seen in Figure 10.

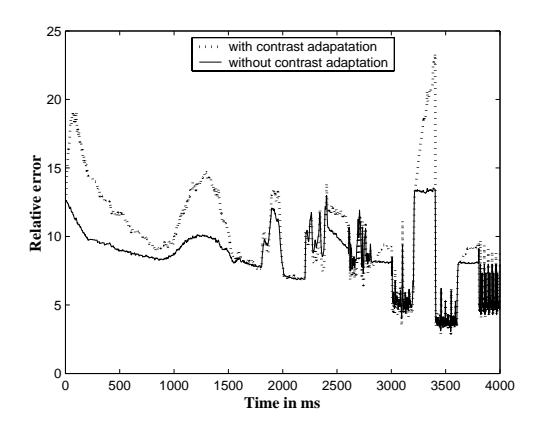


Fig. 10. The simulated relative error of one row of the EMD array of the elaborated EMD model with adaptation is compared to that of the elaborated EMD model without adaptation. It is seen that even though adaptation reduces the dependence of the response to contrast, it increases the relative error.

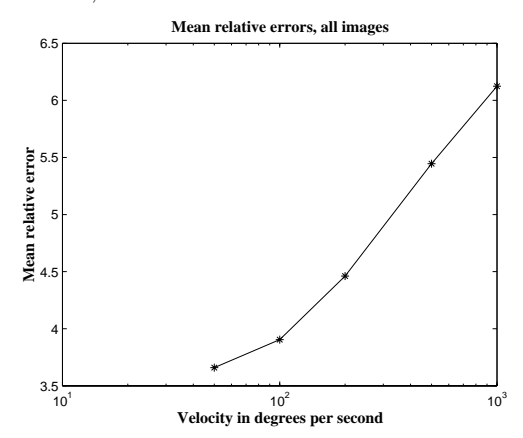


Fig. 11. This figure shows the simulated mean relative error of total elaborated EMD array model including feedback adaptation with the response averaged over 4 images, at 5 different speeds. It is seen that averaging of all the rows of EMDs (spatial integration at the output) reduces the relative error that is shown Figure 10, where only one row of EMDs are taken. It is seen that even though adaptation reduces the dependence of the response to contrast, it increases the relative error and the relative error increases with increase in the velocity because adaptation introduces more variation in the correlator response and hence more errors at higher velocities.

7.1. Saturation

Both simple and elaborated Reichardt correlators show an increase of response amplitude with stimulus contrast. The neural and behavioral responses of the fly display such a dependence only at very low contrasts. As contrast increases above a few percent, the response begins to level off due to a static, compressive non-linearity which is termed as contrast saturation.¹⁴ This is due to limitations in the range of responses that can be signaled by physiological mechanisms. In our model, to further decrease the dependance of the response to contrast, we have implemented saturation at the photoreceptor output and at the correlator arms.

7.2. Saturation at the correlator input

Saturation of the visual signal first occurs in the photoreceptors, which respond roughly to logarithm of luminance.¹⁸ Saturation reduces relative error partly by reducing contrast difference from one region of the image to another. It is seen in flies that this saturation occurs primarily after linear pre-filtering but before

Proc. of SPIE Vol. 5275

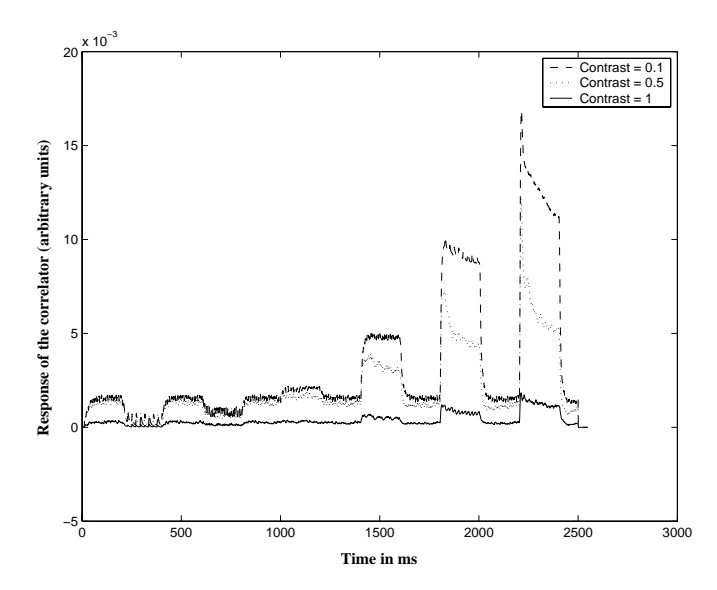


Figure 12. The simulated mean correlator response of one row of EMDs for three different contrast (1, 0.5 and 0.1) including saturation at the photoreceptors and feedback contrast adaptation is shown here. It is seen that due to the saturation effects, the correlator response is squashed and the response increases at low contrasts. It is also seen that the dependence of the response on contrast is further reduced by adding input saturation along with adaptation.

the multiplication operation indicating that contrast saturation must take place after elimination of the mean light intensity from the signal.^{5, 14, 36} Saturation is modelled here by including a compressive non-linearity such as a hyperbolic tangent function of the form, $\rho(C) = \tanh(C)$.

In our model, we have implemented saturation on the spatially pre-filtered input. The effect of this saturation and adaptation on our model is shown in the Figure 12 and Figure 13.

Figure 12 shows the mean response of one row of EMDs for three different contrasts (1, 0.5 and 0.1) including saturation at the photoreceptors and feedback contrast adaptation. The simulation is performed on one image, image1, moving at low adapting speed of 5 degrees per second. The saturation compresses the correlator response and the effect of saturation causes the response to increase with decrease in contrast. It is also seen that the addition of input saturation to adaptation further reduces the dependence of the response to contrast.

Figure 13 shows and the simulated mean relative error of the elaborated EMD model with input saturation and adaptation obtained by testing the model over 4 different images given in Figure 2. It is seen that the relative error is greatly reduced by the addition of saturation (compressive nonlinearity) at the input along with adaptation.

7.3. Saturation at the correlator arms

It is also seen that saturation also takes place on both the delayed and undelayed arms of the correlator with saturation on the delayed arm following the delay filter.^{5, 14} So based on this, we have implemented compressive nonlinearity before the multiplication operation on both correlator arms.

Figure 14 shows the simulated mean corrlator response of one row of EMDs for three different contrast (1, 0.5 and 0.1) including saturation at the correlator arms, saturation at the photoreceptors and feedback contrast adaptation. As expected, due to the saturation effects, the response is higher at lower contrasts and the dependance of the response on contrast is further reduced. The correlator response is further squashed due to the additional compressive non linearity added. Figure 15 compares the simulated mean response of one row of EMDs of an elaborated model with feedback adaptation and saturation at the photoreceptors with

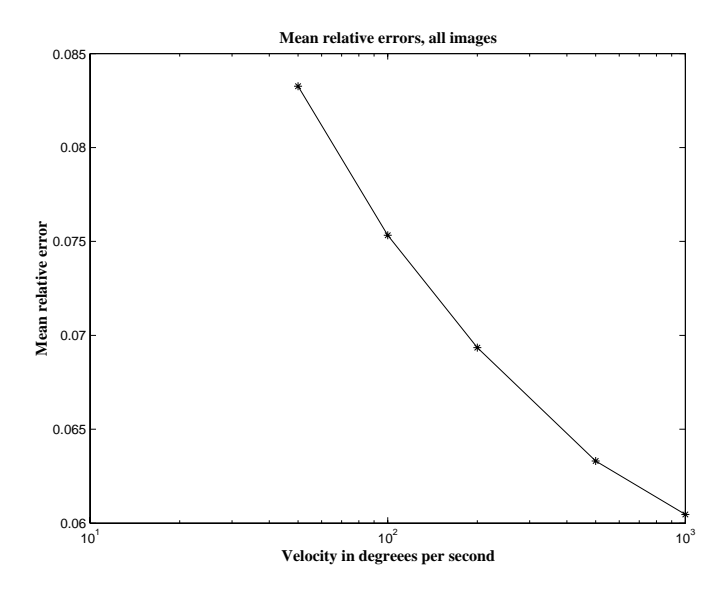


Fig. 13. This figure shows the simulated mean relative error of the elaborated EMD array model including feedback adaptation and input saturation with the response averaged over 4 images, at 5 different speeds. The relative error is greatly reduced by the addition of saturation (compressive nonlinearity) at the input along with adaptation.

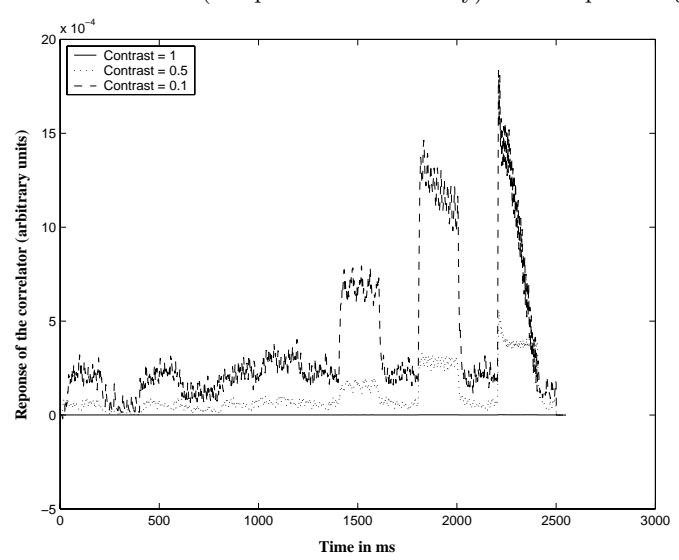


Figure 14. The simulated mean corrlator response of one row of EMDs for three different contrast (1, 0.5 and 0.1) including saturation at the correlator arms, saturation at the photoreceptors and feedback contrast adaptation is shown here. Due to the saturation effects, the response is higher at lower contrasts and the dependance of the response on contrast is further reduced. The correlator response is further squashed due to the additional compressive non-linearity.

that of the elaborated model including feedback adaptation, saturation at the input and saturation at both the correlator arms. The addition of compressive non-linearity further squashes the response of the correlator

8. ELABORATED EMD MODEL WITH ADAPTATION AND SATURATION

Figure 16 shows the block diagram of an elaborated EMD model with adaptation and saturation. The saturation is implemented on the spatially filtered input and at the correlator arms. The feedback signal fed to the

Proc. of SPIE Vol. 5275

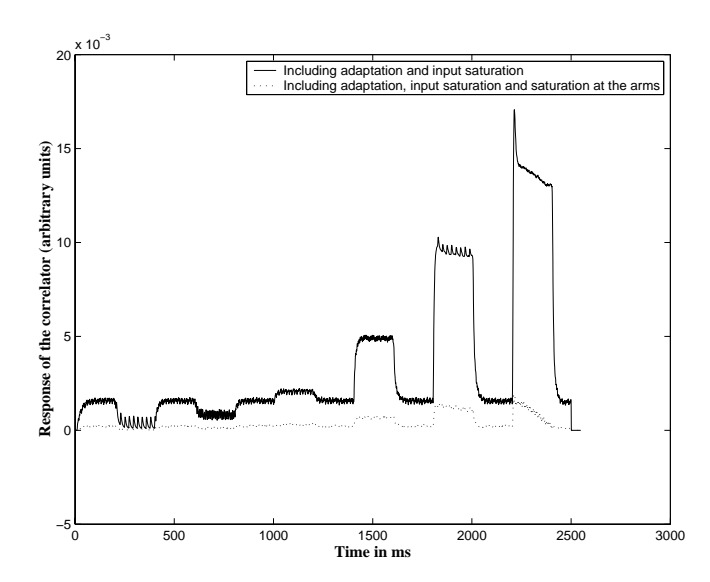


Figure 15. This figure compares the simulated mean response of one row of EMDs of an elaborated model (at contrast = 0.1) with feedback adaptation and saturation at the photoreceptors with that of the elaborated model including feedback adaptation, saturation at the input and saturation at both the correlator arms. It is seen that the addition of compressive non-linearity further squashes the response of the correlator.

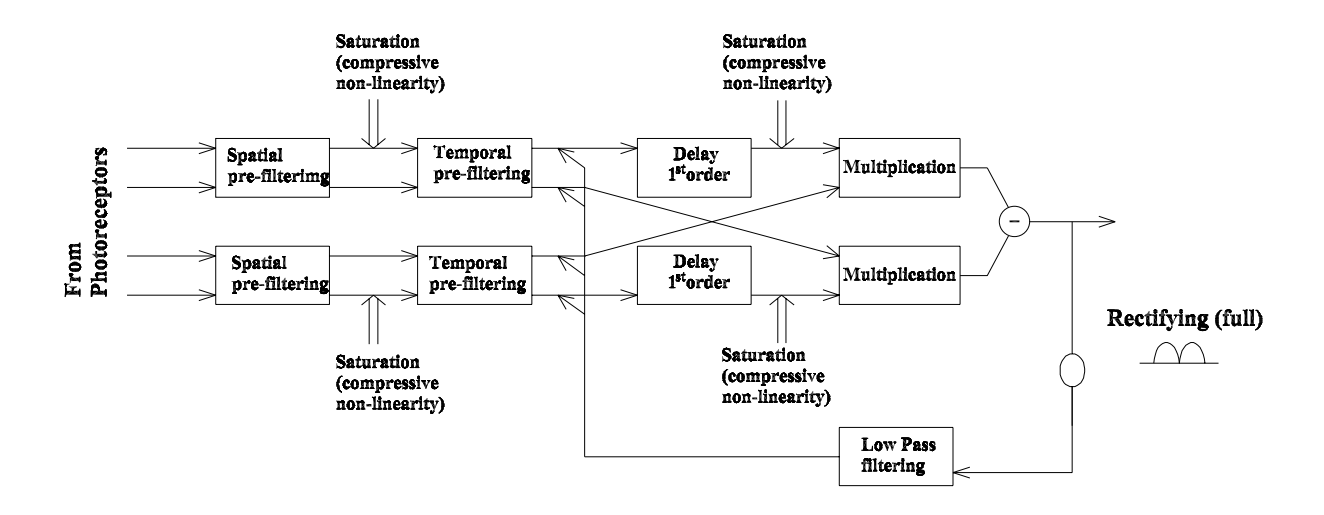


Figure 16. Block diagram of an elaborated EMD model including feedback adaptation and saturation. The saturation is implemented on the spatially filtered input and at the correlator arms.

correlator arms is given by

$$S_{fb} = 1 - (tanh(G_b * (EMD_{out}^3)))$$

Where EMD_{out} is the rectified and low pass filtered output of the EMD and G_b is a constant which we call the feedback gain.

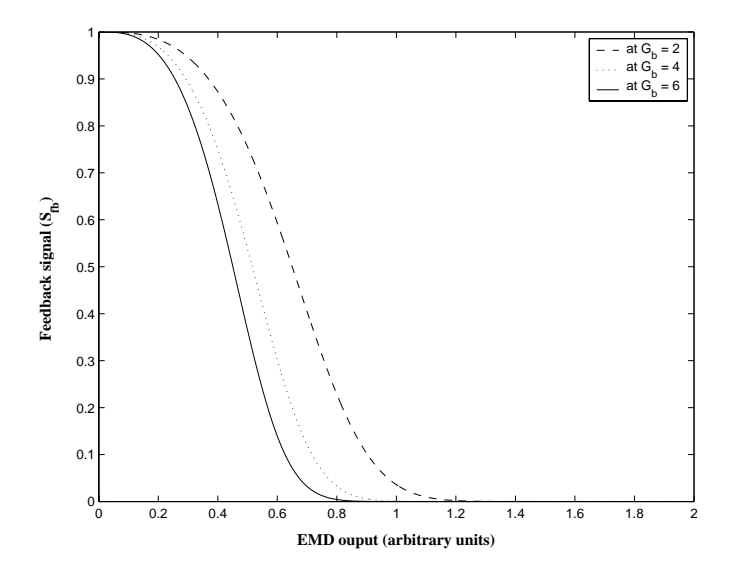


Figure 17. The variation of feedback signal (S_{fb}) as the correlator output is increased is shown here. It is seen clearly at very low response, our elaborated model behaves like a simple correlator. But as the correlator response increases the feedback signal decreases and then eventually becomes zero at high EMD outputs. The response of the feedback signal at three values of G_b (2,4 and 6) are shown here. As the feedback gain increases, the curve shifts to the left and the starts becoming more linear and the response of the feedback signal falls to zero at lower values.

The variation of the feedback signal as the feedback gain is increased is shown in Figure 17. It is seen clearly that at very low response, our elaborated model behaves like a simple correlator. But as the correlator response increases the feedback signal decreases and then eventually becomes zero at high EMD outputs. The response of the feedback signal at three values of G_b (2,4 and 6) are also shown. As the feedback gain increases, the curve shifts to the left and starts becoming more linear and the response of the feedback signal falls to zero at lower values.

Figure 18 shows the simulated mean relative error of the elaborated EMD model with all elaborations obtained by testing the model over 4 different images given in Figure 2. Even though the relative error goes slightly higher by adding the saturation at the correlator arms, the addition of it further decreases the dependance of the response to contrast as is seen in Figure 15.

Hence from all these figures it is seen that the addition of the various elaborations to the Reichardt correlator decreases the dependence of the response to contrast and lowers the relative error. In order to have a better understanding of the saturation effects on the fly visual system, physiological experiments are being done in our lab and based on these physiological results we are hoping to come up with a fully contrast independent model.

9. CONCLUSION

The main idea of this study is to develop an elaborated EMD array model capable of accurate velocity estimation. Although the model does not in its present form, achieve 'velocity constancy' with respect to contrast, as implied by pilot experiments on the fly HS neurons, the model shows reduced effect of contrast on the correlator response.

The comparative study of the effects of the elaborations and the study of the relative error provides us with an insight of how to further improve the model, based on the physiological study of the fly visual system. Ongoing physiological experiments in the lab will further explore the performance of our model and we are expecting that a comparison of the performance of the insect eye and our model to the same stimuli, will help us to achieve a biomimetic model capable of estimating velocity accurately.

Proc. of SPIE Vol. 5275

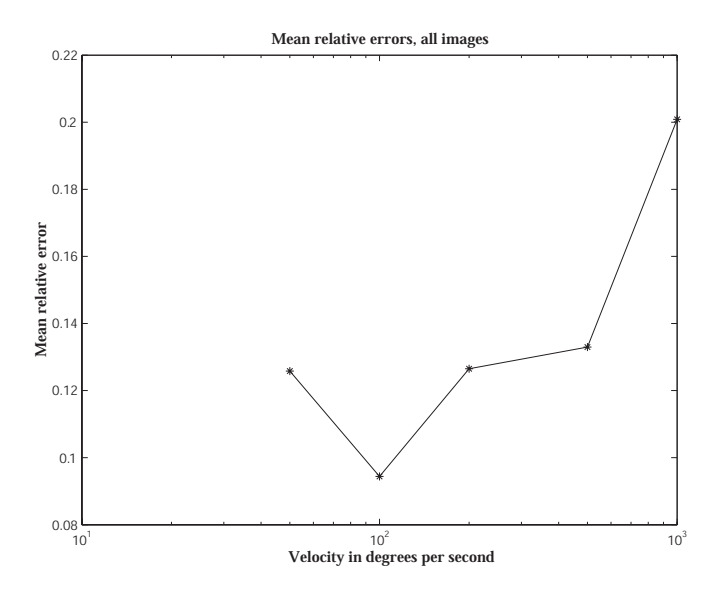


Fig. 18. This figure shows the simulated mean relative error of total elaborated EMD array model including feedback adaptation, input saturation and saturation at the correlator arms with the response averaged over 4 images, at 5 different speeds.

ACKNOWLEDGMENTS

This research is supported by funding from the US Air force Office for Scientific Research / Asian Office for Aerospace Research & Development (contract # F62562-01-P-0158), the Sir Ross & Sir Keith Smith Fund and the Australian Research Council.

REFERENCES

- 1. E. Buchner, "Elementary movement detectors in an insect visual system," *Biological Cybernetics* **24**, pp. 85–101, 1976.
- 2. K. Hausen and M. Egelhaaf, Neural mechanisms of visual course control in insects, *Facets in vision*, edited by R. Hardie and D. Stavenga, Springer-Verlag, Berlin, 1989.
- 3. E. H. Adelson and J. Bergen, "Spatiotemporal energy models for the perception of motion," *Journal of the Optical Society of America A* 2, pp. 284–299, 1985.
- 4. M. V. Srinivasan, J. S. Chahl, K. Weber, S. Venkatesh, M. G. Nagle, and S. W. Zhang, "Robot navigation inspired by principles of insect vision," *Robotics and Autonomous Systems* **26**, pp. 203–216, 1998.
- 5. M. Egelhaaf, A. Borst, and W. Reichardt, "Computational structure of a biological motion detection system as revealed by local detector analysis in the fly's nervous system," *Journal of the Optical Society of America A* 6, pp. 1070–1087, 1989.
- 6. B. Hassenstein and W. Reichardt, "Structure of a mechanism of perception of optical movement," Proceedings of the 1st International Conference on Cybernetics, pp. 797–801, 1956.
- 7. R. O. Dror, D. C. O'Carroll, and S. B. Laughlin, "The role of natural image statistics in biological motion estimation," *Proceedings of the IEEE International Workshop on Biologically Motivated Computer Vision*, Seoul, Korea **1811**, pp. 492–501, 2000.
- 8. H. B. Barlow and W. R. Lewick, "The mechanism of directionally selective units in the rabbit's retina," *Journal of Physiology*, London **178**, pp. 477–504, 1965.
- 9. B. K. P. Horn and B. G. Schunck, "Determining optical flow," *Artificial Intelligence* 17, pp. 185–203, 1981.

- 10. R. B. Pinter, "Adaptation of receptive field spatial organization via multiplicative lateral inhibition," *Proceedings of the the IEEE Conference on Systems, Man and Cybernetics*, pp. 328–331, 1984.
- F. Ratliff and H. K. Hartline, Studies on Excitation and Inhibition in Retina, Chapman and Hall, London, 1974.
- 12. J. P. H. van Santen and G. Sperling, "Elaborated reichardt dtetectors," *Journal of the Optical Society of America A* 2, pp. 300–321, 1985.
- 13. S. H. Courellis and V. Z. Marmarelis, "An artificial neural network for motion detection and speed estimation," *Proceedings of the International Joint Conference on Neural Networks*, pp. 407–421, 1990.
- 14. R. O. Dror, "Accuracy of visual velocity estimation by Reichardt correlators," Master's thesis, University of Cambridge, Cambridge, UK, 1998.
- 15. M. V. Srinivasan, S. W. Zhang, M. Lehrer, and T. S. Collet, "Honeybee navigation en route to the goal: visual flight control and odometry," *Journal of Experimental Biology* **199**, pp. 237–244, 1996.
- 16. S. P. McKee, G. H. Silverman, and K. Nakayama, "Precise velocity discrimination despite random variation in temporal frequency and contrast," *Vision Research* **26**, pp. 609–619, 1986.
- 17. R. O. Dror, D. C. O'Carroll, and S. B. Laughlin, "Accuracy of velocity estimation by Reichardt correlators," *Journal of the Optical Society of America A* 18, pp. 241–252, February 2001.
- 18. S. B. Laughlin, "Matching coding, circuits, cells and molecules to signals: general principles of retinal design in the fly's eye," *Progress in Retinal Research* **13**, pp. 165–195, 1994.
- 19. M. Egelhaaf and A. Borst, "Transient and steady state response properties of movement detectors," Journal of the Optical Society of America A 6, pp. 116–127, 1989.
- S. Single and A. Borst, "Dendritic integration and its role in computing image velocity," Science 281, pp. 1848–1850, 1998.
- 21. T. Maddess and S. B. Laughlin, "Adaptation of the motion sensitive neuron h1 is generated locally and governed by contrast frequency," *Proceedings of the Royal Society of London B* **225**, pp. 251–275, 1985.
- 22. R. A. Harris, D. C. O'Carroll, and S. B. Laughlin, "Adaptation and the temporal delay filter of fly motion detectors," *Vision Research* **39**, pp. 2603–2613, 1999.
- 23. D. L. Ruderman, "The statistics of natural images," *Network: Computation in Neural System* 5, pp. 517–548, 1994.
- 24. A. W. Snyder, D. G. Stavenga, and S. B. Laughlin, "Spatial information capacity of compound eyes," *Journal of Comparative Physiology* **116**, pp. 183–207, 1977.
- 25. A. C. James, White-Noise Studies in the Fly Lamina. PhD thesis, Australian National University, 1990.
- 26. R. C. Hardie, "Functional organisation of the fly retina," Progress in sensory physiology 5, pp. 1–80, 1985.
- 27. R. Payne and J. Howard, "Response of an insect photoreceptor: a simple log-normal model," *Nature* **290**, pp. 415–416, 1981.
- 28. A. C. James, Nonlinear operator network models of processing in the fly lamina, Nonlinear Vision, edited by R. B. Pinter and B. Nabet, CRC Press and Boca Raton, 1992.
- 29. J. H. Howard, A. Dubs, and R. Payne, "The dynamics of phototransduction in insects," *Journal of Comparative Physiology* **154**, pp. 707–718, 1984.
- 30. J. K. Douglass and N. J. Strausfeld, "Visual motion detection circuits in flies: peripheral motion computation by identified small-field retinotopic neurons," *Journal of Neuroscience* **15**, pp. 5596–5611, 1995.
- W. Reichardt, Sensory Communications, edited by A. Rosenblith, MIT Press and John Wiley and Sons, New York, 1961.
- 32. J. P. van Santen and G. Sperling, "Elaborated Reichardt detectors," *Journal of the Optical Society of America A* 2, pp. 300–321, 1985.
- 33. A. Borst and M. Egelhaaf, "Principles of visual motion detection," *Trends In Neurosciences* **12**, pp. 297–306, 1989.
- 34. A. Borst and M. Egelhaaf, "Dendritic processing of synaptic information by sensory interneurons," *Trends In Neurosciences* **17**, pp. 257–263, 1994.

302 Proc. of SPIE Vol. 5275

- 35. R. A. Harris, D. C. O'Carroll, and S. B. Laughlin, "Contrast gain reduction in fly motion adaptation," *Neuron* 28, pp. 595–606, November 2000.
- 36. J. Allik and A. Pulver, "Contrast response of a movement-encoding system," *Journal of Optical Society of America A* 12, pp. 1185–1197, 1995.